Relativistic mean field in $A \approx 80$ nuclei and low-energy proton reactions

Chirashree Lahiri and G. Gangopadhyay
Department of Physics, University of Calcutta, 92 Acharya Prafulla Chandra Road, Kolkata 700 009, India
(Received 21 July 2011; published 11 November 2011)

Relativistic mean-field calculations were performed for a number of nuclei in the mass $A \sim 80$ region. Ground-state binding energy, charge radius, and charge density values were compared with experiment. The optical potential was generated folding the nuclear density with the microscopic nuclear interaction DDM3Y. S factors for low-energy (p,γ) and (p,n) reactions were calculated and compared with experiment.

DOI: 10.1103/PhysRevC.84.057601 PACS number(s): 24.10.Ht, 25.40.Lw, 25.40.Kv, 27.50.+e

The relativistic mean-field (RMF) approach has proved to be very successful in explaining different features of stable and exotic nuclei like ground-state binding energy, deformation, radius, excited states, spin-orbit splitting, neutron halo, etc. [1]. In particular, the radius and the nuclear density are known to be well reproduced. This has led to its application to nuclear reactions also.

Low-energy reactions are very important from the astrophysical point of view. In astrophysical environments, neutron and proton reactions are the keys to nucleosynthesis of heavy elements. The $A \approx 80$ region is an interesting one as (p,γ) and (n,p) reactions play important roles in determining the abundance of elements. In this mass region, there are some proton-rich naturally occurring isotopes of elements known as p nuclei which cannot be produced via the s or r process. Mainly, proton-capture reactions contribute to the formation of such nuclei. Recent works (see, e.g., Ref. [2]) have emphasized the importance of a number of charge exchange reactions in this mass region for production of very light p nuclei. The relevant astrophysical rates can directly be derived from the (p,n) data, although the target is in the ground state and reaction has negative a Q value [3]. A number of recent experiments has focused on reactions using protons having an energy of a few MeV in the $A \approx 80$ region.

Calculation of isotopic abundance requires a network calculation involving many thousands of reactions. Despite the importance of (p,γ) or (p,n) reactions in explaining the abundance of p nuclei, experimental data are rather scarce due unavailability of the target nuclei on Earth. Thus, one often has to depend on theory for these reactions. The calculations essentially utilize the Hauser-Feshbach formalism where, the optical model potential, a key ingredient, is often taken in a local or a global form. It is also possible to use a microscopic optical potential constructed utilizing nuclear densities. If the target is stable, the density of the nucleus is available through electron scattering. However, in the absence of a stable target, theory remains our sole guide to describe the density. Thus, it is imperative to test the theoretical calculations, where experimental data are available, to verify its applicability. We aim to check the success of microscopic optical potentials based on mean-field densities in explaining the reaction cross sections. A good description depending essentially on theory will allow one to extend the present method to the critical reactions that are beyond present day laboratory capabilities.

Calculations using microscopic potentials have been able to explain the observed elastic-scattering cross sections even in nuclei far from the stability valley (See, *e.g.* Ref. [4] and references therein). Low-energy projectiles probe only the outermost regions of the target nuclei. Hence, the nuclear skin plays a very important role in such reactions. The density information should be available from theoretical calculations. This method has been utilized to study low-energy proton-capture reactions in Ni and Cu nuclei [5] and nuclei in the $A = 60$–80 region [6].

For the present study we have selected a number of low-energy proton reactions for their astrophysical relevance. The reactions $^{84,86,87}\mathrm{Sr}(p,\gamma)$ were investigated through an activation technique by Gyürky *et al.* in Ref. [7]. It is important to note that ^{84}Sr is another p nucleus. In beam measurements were performed by Galanopoulos *et al.* [8] to find out the cross sections for the reaction $^{88}\mathrm{Sr}(p,\gamma)$. As for charge exchange reactions, three reactions, identified as important by Rapp *et al.* [2] and for which experimental cross sections are available, have been selected for study. The reaction $^{75}\mathrm{As}(p,n)$ was studied in Refs. [9–11] through in-beam detection of neutrons. Finally, the reactions $^{76}\mathrm{Ge}(p,n)$ [12] and $^{85}\mathrm{Rb}(p,n)$ [3] were studied by use of the activation technique. In the present work, we investigate the reactions mentioned above in a microscopic approach.

Theoretical density profiles were extracted in the RMF approach. There are different variations of the Lagrangian density as well as a number of different parametrizations. In the present work we have employed the FSU Gold [13] Lagrangian density. It contains, apart from the usual terms for a nucleon-meson system, nonlinear terms involving self-coupling of scalar-isoscalar mesons and additional terms describing self-coupling of the vector-isoscalar meson and coupling between the vector-isoscalar meson and the vector-isovector meson.

Pairing has been introduced under the BCS approximation using a zero-range pairing force of strength 300 MeV-fm for both proton and neutrons. The RMF + BCS equations are solved under the usual assumptions of classical meson fields, time-reversal symmetry, no-sea contributions, and so on. Since we need the densities in coordinate space, the Dirac and the Klein Gordon equations have directly been solved in that space. This approach has earlier been used [4,14,15] in neutron-rich nuclei in different mass regions.

The microscopic optical model potentials for the reactions are obtained using effective interactions derived from the

 ©2011 American Physical Society

nuclear matter calculation in the local density approximation, i.e., by substituting the nuclear matter density with the density distribution of the finite nucleus. In the present work, the microscopic nuclear potentials have been constructed by folding the density-dependent DDM3Y [16,17] effective interaction with the densities from the RMF calculation. This interaction, obtained from a finite-range energy-independent M3Y interaction by adding a zero-range energy-dependent pseudopotential and introducing a density-dependent factor, has been employed successfully in nucleon nucleus as well as nucleus nucleus scattering, calculation of proton radioactivity, and so on. The density dependence has been chosen in the form $C(1 - \beta\rho^{2/3})$ [17], the constants being obtained from a nuclear matter calculation [18]. The real and the imaginary parts of the potential are taken as 0.7 times and 0.1 times the DDM3Y potential, respectively. This normalization have also been used in our earlier work on (p,γ) reactions in lighter nuclei [6]. We have checked that the above values adequately describe the cross-section measurements. Of course, these parameters can be tuned to fit the cross sections in individual reactions. For example, in ^{84}Sr, if we choose the imaginary part of the potential as 0.3 times the DDM3Y potential, the result will differ by 10% and fit the experimental data better. However, we believe that a single parametrization for the entire mass region is more useful.

The Coulomb potentials are similarly constructed by folding the Coulomb interaction with the microscopic proton densities. We have already used such potentials to calculate life times for proton, α, and cluster radioactivity [19] as well as elastic proton scattering [4] in different mass regions of the periodic table.

Reaction calculations have been performed with the computer code TALYS 1.2 [20] assuming spherical symmetry for the target nuclei. The DDM3Y interaction is not a standard input of TALYS but can easily be incorporated. Though the nuclear matter-nucleon potential does not include a spin-orbit term, the code provides a spin-orbit potential from the Scheerbaum prescription [21] coupled with the phenomenological complex potential depths. The default form for this potential given in the code has been used without any modification.

The TALYS code has a number of other useful features. We have employed the full Hauser-Feshbach calculation with transmission coefficients averaged over total angular-momentum values and with corrections due to width fluctuations. Up to 30 discrete levels of the nuclei involved have been included in the calculation.

Our calculations, being more microscopic, are more restricting. Yet, the rate depends on the models of the level density and the $E1$ γ strength function adopted in the calculation of cross sections. Phenomenological models are usually fine tuned for nuclei near the stability valley. Microscopic prescriptions, on the other hand, can be extended to the drip lines and, hence, have been assumed in all nuclei. We have calculated our results with microscopic level densities in Hartree-Fock (HF) and Hartree-Fock-Bogoliubov (HFB) methods, calculated in TALYS by Goriley and Hilaire, respectively. We have also compared our results using phenomenological level densities from a constant-temperature Fermi gas model, a back-shifted Fermi gas model, and a generalized superfluid model from TALYS. The cross sections are very much dependent on the level density chosen, sometimes changing by a factor of 50%. We find that, in most the cases, the HFB densities fit the experimental data better in our formalism.

TABLE I. Experimental binding energy and charge radii values compared with calculated results.

	B.E. (MeV)		r_{ch}(fm)	
	Expt.	Theor.	Expt.	Theor.
^{84}Sr	728.90	727.53	4.236	4.232
^{86}Sr	748.93	748.27	4.226	4.240
^{87}Sr	757.36	757.17	4.220	4.245
^{88}Sr	768.47	768.47[a]	4.220	4.249
^{75}As	652.56	652.38	4.097	4.082
^{76}Ge	661.60	660.69	4.081	4.053
^{85}Rb	739.28	738.70	4.203	4.218

[a]Normalized following the prescription of Refs. [22,23].

For $E1$ γ strength functions, results derived from HF + BCS and HFB calculations, available in the TALYS database, were employed. In agreement with our observation in Ref. [6], the results for HFB calculations describe the S factors reasonably well and we present our results for that approach only.

It is possible to scale the theoretical capture cross sections to match with experiment using a parameter G_{norm} in the code used to scale the γ-ray transmission coefficient. However, for the present paper, we have not scaled the theoretical results. All the parameters in the Lagrangian density and the interaction are standard ones and have not been changed.

As the density profile is the important quantity in our formalism, a comparison of the radii values can provide some idea about the agreement of the calculated densities with experiments. In Table I, we compare our results for the binding energy and charge radii (r_{ch}) with measurements for those nuclei in this mass region, which have been used as targets for low-energy proton-capture or charge-exchange reactions. The binding energy values from the mean-field approach have been corrected using the formalism developed in Refs. [22,23]. The experimental binding energy values are from Ref. [24].

Charge radii have been calculated from the charge densities, which, in turn, have been obtained from the calculated point proton density ρ_p by taking into account the finite size of the proton. The point proton density is convoluted with a Gaussian form factor $g(\mathbf{r})$,

$$\rho_{ch}(\mathbf{r}) = \int e\rho_p(\mathbf{r}')g(\mathbf{r} - \mathbf{r}')d\mathbf{r}' \quad (1)$$

$$g(\mathbf{r}) = (a\sqrt{\pi})^{-3}\exp(-r^2/a^2) \quad (2)$$

with $a = 0.8$ fm.

Experimental charge radii values are from Angeli [25]. The results show that RMF can describe the charge radii of these nuclei with sufficient accuracy. One sees that in most of the nuclei, the difference between measurement and theory is less than 1%.

Direct comparison of charge density is more difficult in absence of accurate experimental information. De Vries

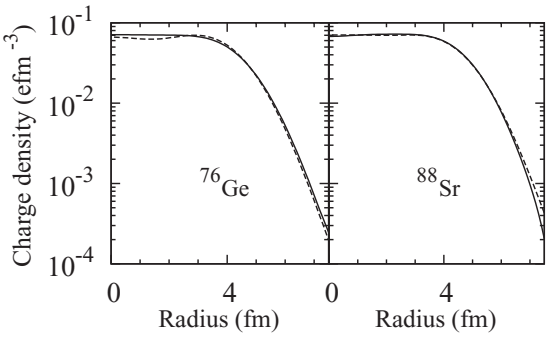

FIG. 1. Comparison of charge density obtained from Fourier-Bessel analysis of experimental electron scattering data (solid line) and calculated in the present work (dashed line).

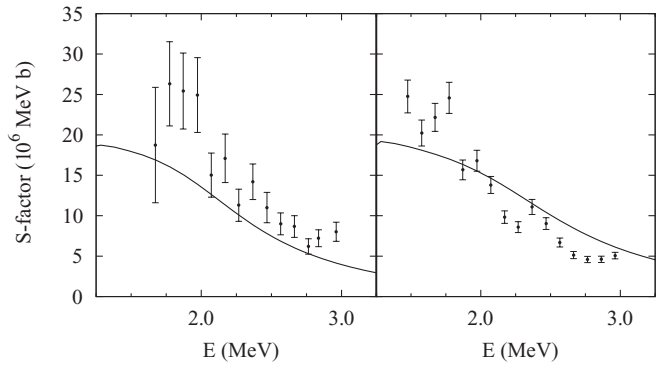

FIG. 2. Experimental and calculated S factors for (p,γ) reactions in (a)^{84}Sr and (b) ^{86}Sr targets.

et al. [26] have presented the coefficients of Fourier-Bessel expansion for charge density of a number on nuclei extracted from electron-scattering data. It includes two nuclei of our interest, ^{76}Ge and ^{88}Sr. In Fig. 1, we compare the charge density extracted from the Fourier-Bessel coefficients and our calculated results for the above two nuclei. One can see that the theoretical and experimental values agree very well, particularly at larger radii values, which is the region expected to contribute to the optical potential at low projectile energy. However, in absence of information on error in the density values, this conclusion can remain only tentative.

We then compare the results for the reaction calculation in the above-mentioned reactions with experiments. As the astrophysically important Gamow window lies in the region 1.3 to 3.9 MeV for these nuclei, we present the results covering this energy region. The cross section varies very rapidly at such low energy, making comparison between theory and experiment rather difficult. The usual practice in low-energy nuclear reaction is to compare another key observable, viz. the S factor. The expression of the astrophysical S factor [6] is given by

$$S(E) = E\sigma(E)e^{2\pi\eta}, \tag{3}$$

where E is the energy in center-of-mass frame in KeV, $\sigma(E)$ is the reaction cross section in barns, and η indicates the Sommerfeld parameter with $2\pi\eta = 31.29Z_pZ_t\sqrt{\mu/E}$. Here, Z_p and Z_t are the charge numbers of the projectile and the target, respectively, and μ is the reduced mass (in amu). It varies much more slowly than reaction cross sections as the exponential energy dependence of cross section is not present in it. For this reason, we calculate this quantity and compare it with experimentally extracted values.

Figures 2 and 3 show the results for the reactions $^{84,86-88}$Sr(p,γ). The results compare favorably with experiments compared to the NON-SMOKER code calculations of Rauscher *et al*. [27]. However, it needs to be pointed out that, in the case of ^{87}Sr, theoretical results overpredict the cross-section values. It was suggested [7] that perhaps the agreement with theory (in their case the NON-SMOKER calculation) worsens as one goes to more neutron-rich nuclei. However, as one can see in the right panel of Fig. 2, this trend is not shared by the present calculation.

Figure 3 shows the results for the (p,n) reactions on (a) ^{75}As, (b) ^{76}Ge, and (c) ^{85}Rb targets. These reactions (along with their inverse reactions) are listed among the 10 most important reactions in deciding the abundance of the p nuclei in Rapp *et al*. [2]. The three measurements for the ^{75}As(p,n) reaction are rather old and error values are not available for most of the measurements. The quoted error in cross section is 10% or above. In ^{76}Ge, we find that the calculation systematically overpredict the results by as much as 60%. On the other hand, the calculations for the ^{85}Rb(p,n) reaction produce excellent match with experimental measurements.

We find that our calculation can reproduce the S-factor values with reasonable success. Even in the worst case, the calculation is off by a factor of less than 2 while the cross-section values range over four orders of magnitude. However, one should remember that in astrophysical calculations, the rates are often varied by a large factor, viz. 10 or 100 [2]. Thus, the present microscopic calculations can be used to obtain rates which are dependable for astrophysical calculations.

We point out that, in our earlier work [5], we have showed that the default local and global optical potentials [28] in the TALYS package also can be used with suitable normalization of γ-ray strength to produce comparable results for certain energy ranges. In the present case also, suitable selection of the parameter brings the values calculated with default potential close to experimental values. However, we believe

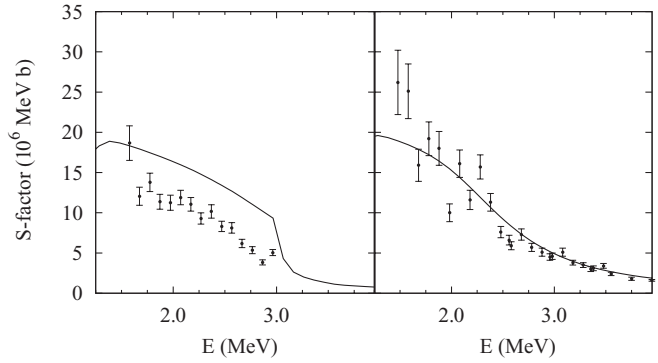

FIG. 3. Experimental and calculated S factors for (p,γ) reactions in (a)^{87}Sr and (b) ^{88}Sr targets.

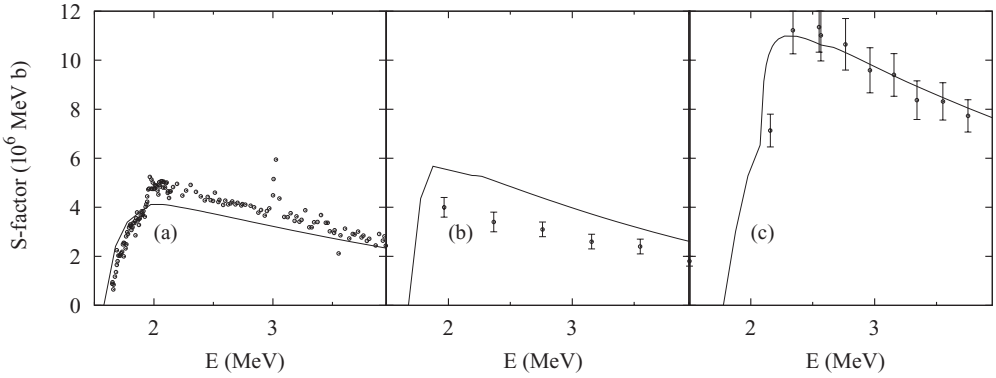

FIG. 4. Experimental and calculated S factors for (a) ^{75}As(p,n), (b) ^{76}Ge(p,n), and (c) ^{85}Rb(p,n) reactions, respectively.

that the present microscopic approach is more suitable, as no normalization is necessary, and the method can be extended to reactions where experimental data are not available.

In summary, cross sections for low-energy (p,γ) and (p,n) reactions for a number of nuclei in $A \approx 80$ region in the energy regime important for explosive nucleosynthesis have been calculated using the TALYS code. The microscopic optical potential has been obtained by folding the DDM3Y microscopic interaction with the nuclear densities obtained from RMF calculation using the Lagrangian density FSU Gold.

This work was carried out with financial assistance of the UGC-sponsored DRS Programme of the Department of Physics of the University of Calcutta. C.L. acknowledges a grant from the UGC. G.G. gratefully acknowledges the hospitality of the ICTP, Trieste, where a part of the work was carried out.

[1] See, e.g., P. Ring, Prog. Part. Nucl. Phys. **37**, 193 (1996).
[2] W. Rapp *et al.*, Astrophys J. **653**, 474 (2006).
[3] G. G. Kiss *et al.*, Phys. Rev. Lett. **101**, 191101 (2008); T. Rauscher *et al.*, Phys. Rev. C **80**, 035801 (2009).
[4] G. Gangopadhyay and S. Roy, J. Phys. G: Nucl. Part. Phys. **31**, 1111 (2005).
[5] G. Gangopadhyay, Phys. Rev. C **82**, 027603 (2010).
[6] C. Lahiri and G. Gangopadhyay, Eur. Phys. J. A **47**, 87 (2011).
[7] Gy. Gyürky *et al.*, Phys. Rev. C **64**, 065803 (2001).
[8] S. Galanopoulos *et al.*, Phys. Rev. **67**, 015801 (2003).
[9] C. H. Johnson, A. Galonsky, and J. P. Ulrich, Phys. Rev. **109**, 1243 (1958).
[10] C. H. Johnson, C. Trail, and A. Galonsky, Phys. Rev. B **136**, 1719 (1964).
[11] R. D. Albert, Phys. Rev. **115**, 925 (1959).
[12] G. G. Kiss *et al.*, Phys. Rev. C **76**, 055807 (2007).
[13] B. G. Todd-Rutel and J. Piekarewicz, Phys. Rev. Lett. **95**, 122501 (2005).
[14] M. Bhattacharya and G. Gangopadhyay, Phys. Rev. C **72**, 044318 (2005); Fizika B (Zagreb) **16**, 113 (2007).
[15] M. Bhattacharya and G. Gangopadhyay, Phys. Rev. C **75**, 017301 (2007).
[16] A. M. Kobos *et al.*, Nucl. Phys. A **425**, 205 (1984).
[17] A. K. Chaudhuri, Nucl. Phys. A **449**, 243 (1986); **459**, 417 (1986).
[18] D. N. Basu, J. Phys. G: Nucl. Part. Phys. B **30**, 7 (2004).
[19] G. Gangopadhyay, J. Phys. G: Nucl. Part. Phys. **36**, 095105 (2009), and references therein.
[20] A. J. Koning, S. Hilaire, and M. Duijvestijn, *Proceedings of the International Conference on Nuclear Data for Science and Technology, April 22–27,* 2007, *Nice, France*, edited by O. Bersillon, F. Gunsing, E. Bauge, R. Jacqmin, and S. Leray (EDP Sciences, Paris, 2008), pp. 211–214.
[21] R. R. Scheerbaum, Nucl. Phys. A **257**, 77 (1976).
[22] M. Bhattacharya and G. Gangopadhyay, Phys. Lett. B **672**, 182 (2009).
[23] G. Gangopadhyay, J. Phys. G: Part. Nucl. Phys **37**, 015108 (2010).
[24] G. Audi, A. H. Wapstra, and C. Thibault, Nucl. Phys. A **729**, 337 (2003).
[25] I. Angeli, At. Data Nucl. Data Tables **87**, 185 (2004).
[26] H. De Vries, C. W. De Jager, and C. De Vries, At. Data Nucl. Data Tables **36**, 495 (1987).
[27] T. Rauscher and F.-K. Thielmann, At. Data Nucl. Data Tables **75**, 1 (2000); **76**, 47 (2001).
[28] A. J. Koning and J. P. Delaroche, Nucl. Phys. A **713**, 231 (2003).